AJNR Am J Neuroradiol 25:571–573, April 2004

Technical Note

Three-Dimensional Digital Angiography: New Tool for Simultaneous Three-Dimensional Rendering of Vascular and Osseous Information during Rotational Angiography

Philippe Gailloud, Satoru Oishi, Jeffrey Carpenter, and Kieran J. Murphy

Summary: Three-dimensional (3D) digital subtraction angiography (DSA) is the latest development in the neurovascular imaging armamentarium. 3D-DSA combines the anatomic resolution of DSA with 3D visualization abilities previously offered by only CT or MR angiography. 3D-DSA provides more detailed information than does DSA alone in the evaluation of neurovascular lesions, such as cerebral aneurysms. However, the inability of 3D-DSA to simultaneously image osseous and vascular structures is noted as a weakness of this technique compared with CT angiography. We describe a new 3D digital angiography reconstruction algorithm that allows the concurrent display of the cerebral vasculature and the osseous landmarks.

Despite recent advances in CT angiography and MR angiography, digital subtraction angiography (DSA) remains the criterion standard imaging technique for evaluation of the cerebral vasculature (1). Three-dimensional (3D) reconstruction of the dataset acquired during rotational DSA represents the latest development in the neurovascular imaging armamentarium. This technique combines the anatomic resolution of DSA with the 3D visualization abilities previously offered by only CT or MR angiography and provides more detailed information than does DSA alone in the evaluation of neurovascular lesions, such as cerebral aneurysms (2–5). 3D-DSA has taken a prominent role in treatment planning by enabling better appreciation of the morphology of complex vascular lesions before endovascular or surgical management. It is also superior in the performance of sophisticated tasks such as aneurysm volume measurement (6). On the other hand, the inability of 3D-DSA to simultaneously image osseous and vascular structures is noted as a weakness of this technique compared with CT angiography (1, 7, 8). We describe a new 3D digital angiography (DA) reconstruction algorithm that allows concurrent display of the cerebral vasculature and osseous landmarks.

Received October 1, 2003; accepted after revision November 1.

From the Division of Interventional Neuroradiology (P.G., J.C., K.J.M.), the Johns Hopkins Medical Institutions, Baltimore, MD, and the Toshiba Medical Systems Research and Development Center (S.O.), Tochigi, Japan.

Address reprint requests to Philippe Gailloud, MD, Division of Interventional Neuroradiology, Department of Radiology and Radiological Sciences, the Johns Hopkins Medical Institutions, Baltimore, MD 21287.

Technical Report

Technique

3D-DSA was performed in each patient according to a standard protocol during routine clinical examination. We used a transfemoral arterial approach with a 5F sheath, 5F diagnostic catheters, biplane DSA equipment (Infinix NB; Toshiba, Tochigi, Japan), and nonionic iodinated contrast agent (Omnipaque 300; Amersham Health, Princeton, NJ). Volumes of contrast agent and rates for rotational acquisitions at our institution are as follows: vertebral artery (VA) (18 mL, 3 mL/sec), common carotid artery (24 mL, 4 mL/sec), and internal carotid artery (ICA) (18 mL, 3 mL/sec). Rotational angiographic data were acquired through a 200° rotation of the anteroposterior X-ray tube around the patient's head (angular velocity, 40° per second). A 3D representation of the rotational acquisition was then generated by using commercially available 3D angiography software (Toshiba) and transferred to a computer workstation for postprocessing (Vitrea 2; Vital Images, Plymouth, MN). For each rotational acquisition, both 3D-DSA and 3D-DA reconstructions were obtained.

Case Illustrations

Case 1

In a 36-year-old woman presenting with intracranial hemorrhage, DSA revealed a right occipital arteriovenous malformation (AVM) fed by branches of the left posterior cerebral artery. Rotational angiography of the left VA was performed as part of routine preoperative evaluation of the AVM. Both 3D-DSA and 3D-DA reconstructions were obtained. Figure 1 shows the AVM nidus, its arterial feeders, and draining veins projecting over bony landmarks, which the surgeon later used to plan the operative approach. Figure 1A also illustrates the detailed anatomic and topographic information offered by 3D-DA through its combined rendering of osseous and vascular structures. The left posterior-inferior cerebellar artery (PICA) had a fenestrated origin and crossed the foramen magnum for a short, recurrent, extracranial course. The AICA looped within the left internal auditory canal; this finding was better appreciated on a magnified posteroanterior projection (Fig 1B).

Case 2

DSA was performed as part of the pretreatment evaluation of a 38-year-old woman complaining of a large, pulsatile, subcutaneous occipital mass. Images revealed a suboccipital arteriovenous fistula. Both 3D-DSA and 3D-DA reconstructions

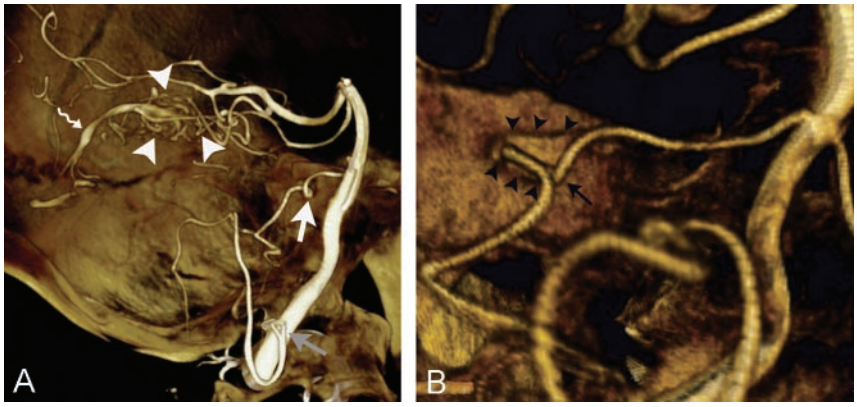

FIG 1. Images obtained in a 36-year-old woman with a right occipital AVM fed by braches of the left posterior cerebral artery. Volume-rendered 3D-DAs from a rotational acquisition in the left VA.

A, Lateral projection shows the small left occipital AVM (*arrowheads*) and its adjacent draining vein (*squiggly arrow*). A curve of the anterior-inferior cerebellar artery (AICA) in the internal auditory canal (*white arrow*) and a fenestrated posterior-inferior cerebellar PICA (*gray arrow*) with an extracranial loop are demonstrated within their surrounding osseous landmarks.

B, Posteroanterior projection shows the intracanalar segment (*arrowheads*) of the left AICA (*arrow*) to better advantage.

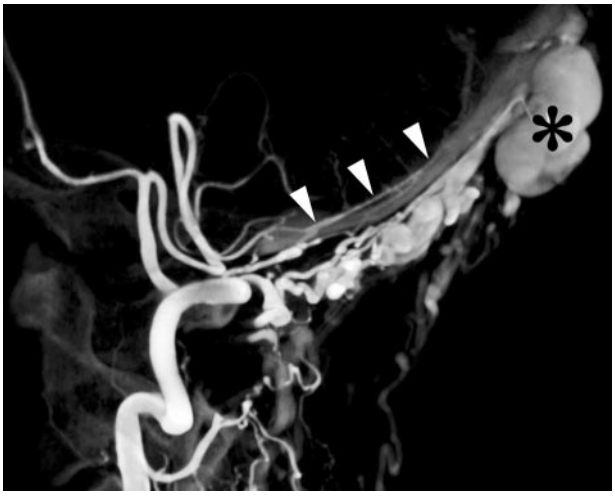

FIG 2. Images in a 38-year-old woman with a suboccipital arteriovenous fistula. Lateral volume-rendered 3D-DA of a left VA rotational acquisition shows the extracalvarial arterial supply coursing along the occipital bone to the scalp arteriovenous fistula. The arterial supply is via C1 and, to a lesser extent, C2 muscular branches of the VA. Note the large occipital varix (*asterisk*). A left posterior meningeal artery (*arrowheads*) is coursing along the inner aspect of the occipital bone, but it does not participate in vascularization of the lesion.

were generated from a rotational acquisition in the left VA, and both provided information about the number, morphology, and origin of the arterial feeders as well as about the configuration of the varix draining the lesion. In addition, 3D-DA precisely delineated the topographic relationship between the vascular components of the malformation and the adjacent occipital bone (Fig 2).

Case 3

This 52-year-old woman had a right distal ICA aneurysm, which was incidentally discovered during MR imaging. DSA confirmed a saccular aneurysm arising from the medial wall of the distal left ICA. Left common carotid rotational angiography was performed, and both 3D-DSA and 3D-DA reconstructions were obtained. Figure 3A is a lateral view of the distal left ICA and shows the relationship of the aneurysm to the surrounding osseous structures. Figure 3B more specifically illustrates the intrasellar location of the aneurysm. Both specimen-like and dry-bone renderings of the 3D images are shown.

Discussion

The 3D reconstruction of a rotational angiographic acquisition, or 3D-DSA, has now become a tool of routine use in the evaluation of the cerebral vasculature. 3D-DSA provides more-detailed vascular information than both standard two-dimensional angiography and rotational angiography (5). The value of 3D-DSA has been demonstrated in the precise evaluation of intracranial aneurysms, where it not only provides exquisitely detailed anatomic information but also helps in choosing the most appropriate working projection for subsequent endovascular therapy (2–4). However, its inability to provide information about osseous structures surrounding the aneurysm is a significant disadvantage compared with CT angiography (1, 7). The 3D angiographic technique described in this report overcomes this drawback of 3D-DSA by simultaneously reconstructing and displaying the osseous and vascular structures obtained from a single nonsubtracted rotational data acquisition. This new technique utilizes the same dataset used to generate the 3D-DSA images. Both types of reconstructions (3D-DSA and 3D-DA) can therefore be obtained from the same rotational image acquisition with a single injection of contrast material.

For 3D-DSA, an initial rotational acquisition is obtained before administration of the contrast agent and serves as a mask sequence for the subsequent subtraction process. A second identical rotational acquisition is performed as the contrast agent selectively flows through the arterial tree of interest. Subtracting the mask images from the contrast-enhanced images with matching angles then creates rotational DSA images. A detailed 3D representation of the vascular tree is finally generated from the rotational DSA dataset by using a 3D reconstruction algorithm based on the Feldkamp method, one of the most commonly used 3D reconstruction algorithms (9). This mode of reconstruction produces the 3D images available on most modem angiographic units.

3D-DA uses only the set of unsubtracted rotational data acquired as the contrast agent flows through the arterial tree. The dataset to be reconstructed therefore contains both vascular and osseous information. Because no subtraction algorithm is applied, the nonuniformity of signal intensity inherent to the imaging

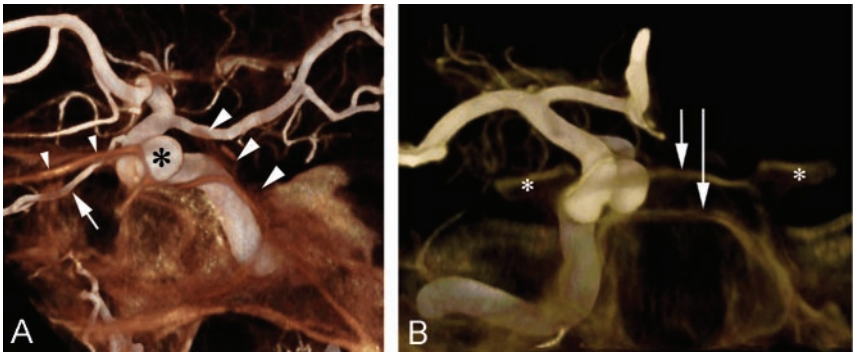

FIG 3. Volume-rendered 3D-DAs of a right common carotid artery rotational acquisition in 52-year-old woman with a right distal ICA aneurysm, which was incidentally discovered.

A, Lateral view shows the distal right ICA in relation to the adjacent skull. The aneurysm in the superior hypophyseal region (*asterisk*) and the right ophthalmic artery (*arrow*) are demonstrated. The relationships of the aneurysm with the clivus (*right arrowheads*) and the jugum sphenoidale (*left arrowheads*) are appreciated. Note the specimen-like rendering.

B, Anteroposterior view shows the distal right ICA in relation to the adjacent skull. This view demonstrates the intrasellar location of the aneurysm, which is lying on the floor of the sella (*long arrow*). Note the jugum sphenoidale (*short arrow*) and the anterior clinoid processes (*asterisk*). Also note the dry-bone rendering.

chain (ie, to the image intensifier and TV system) is not compensated. This artifactual signal intensity causes the periphery of the field of view (FOV) to be darker than its center. To correct this alteration in signal intensity, a flood image must be subtracted from each image of the rotational dataset. Flood images are obtained separately, without phantoms, as part of the monthly calibration of the angiographic equipment. Because flood images are acquired with an empty FOV, they contain only the artifactual signal intensity inhomogeneity created by the imaging chain itself. Subtracting flood images from the rotational dataset therefore eliminates signal-intensity inhomogeneity while retaining both the osseous and vascular information. 3D-DA images are generated from these compensated rotational DA images by using the Feldkamp method. A technical challenge specific to 3D-DA, ie, the inclusion of the osseous frame into the reconstruction dataset, lies in the fact that part of the skull may project outside the FOV on some of the acquired projections. These incomplete projections can cause severe artifacts on the final 3D-DA images. Limiting the reconstruction volume to a sphere projecting onto the FOV on all acquired projections reduces this problem at the cost of the information outside the sphere. We used an alternate method that takes advantage of the entire rotational dataset by applying an extrapolation technique (10) before the reconstruction step.

The inability of CT angiography to clearly demonstrate aneurysms adjacent to osseous structures and fine vascular details, such as the small perforators surrounding an aneurysm, has been noted (7). If the spatial resolution of 3D-DA, which is similar to that of 3D-DSA, allows an analysis of subtle anatomic findings, it shares with CT angiography a relative weakness in adequately imaging structures in the immediate vicinity of bone. Because the 3D-DA reconstruction process is based on electronic manipulation of a single nonsubtracted rotational dataset, opacified blood vessels near or at the contact point of osseous structures of approaching Hounsfield units are difficult to individualize precisely. This is particularly true for the vascular anatomy and pathology of the skull base. This weakness clearly represents an aspect of 3D-DA that can be improved with further refinement of the reconstruction algorithm.

Conclusions

3D-DA is a new reconstruction algorithm that allows simultaneous 3D display of the osseous and vascular information acquired through a rotational cerebral angiogram. Because 3D-DA uses a part of the dataset necessary to generate 3D-DSA images, both 3D-DA and 3D-DSA images can be reconstructed from a single rotational angiogram. The concomitant representation of vascular structures and their osseous environment allows 3D-DA to combine the spatial resolution of 3D-DSA with the topographic information previously offered by only CT angiography.

References

1. Chappell ET, Moure FC, Good MC. **Comparison of computed tomographic angiography with digital subtraction angiography in the diagnosis of cerebral aneurysms: a meta-analysis.** *Neurosurgery* 2003;52:624–631, discussion 630–621
2. Hochmuth A, Spetzger U, Schumacher M. **Comparison of three-dimensional rotational angiography with digital subtraction angiography in the assessment of ruptured cerebral aneurysms.** *AJNR Am J Neuroradiol* 2002;23:1199–1205
3. Hirai T, Korogi Y, Suginohara K, et al. **Clinical usefulness of unsubtracted 3D digital angiography compared with rotational digital angiography in the pretreatment evaluation of intracranial aneurysms.** *AJNR Am J Neuroradiol* 2003;24:1067–1074
4. Abe T, Hirohata M, Tanaka N, et al. **Clinical benefits of rotational 3D angiography in endovascular treatment of ruptured cerebral aneurysm.** *AJNR Am J Neuroradiol* 2002;23:686–688
5. Sugahara T, Korogi Y, Nakashima K, Hamatake S, Honda S, Takahashi M. **Comparison of 2D and 3D digital subtraction angiography in evaluation of intracranial aneurysms.** *AJNR Am J Neuroradiol* 2002;23:1545–1552
6. Piotin M, Gailloud P, Bidaut L, et al. **CT angiography, MR angiography and rotational digital subtraction angiography for volumetric assessment of intracranial aneurysms: an experimental study.** *Neuroradiology* 2003;45:404–409
7. Hirai T, Korogi Y, Ono K, et al. **Preoperative evaluation of intracranial aneurysms: usefulness of intraarterial 3D CT angiography and conventional angiography with a combined unit—initial experience.** *Radiology* 2001;220:499–505
8. Nishihara M, Tamaki N. **Usefulness of volume-rendered three-dimensional computed tomographic angiography for surgical planning in treating unruptured paraclinoid internal carotid artery aneurysms.** *Kobe J Med Sci* 2001;47:221–230
9. Feldkamp LA, Davis LC, Kress JW. **Practical cone-beam algorithm.** *J Opt Soc Am A* 1984;1:612–619
10. Ohishi S, Yamaguchi M, Ohyyama N, Honda T. **Three-dimensional reconstruction from cone-beam projections.** In: Schneider RH, ed. *Medical Imaging V: Image Physics.* SPIE The International Society for Optical Engineering. Bellingham, WA: 1991;280–285